scientific reports

Check for updates

OPEN

Quantum classical hybrid convolutional neural networks for breast cancer diagnosis

Qiuyu Xiang, Dongfen Li✉, Zhikang Hu, Yuhang Yuan, Yuchen Sun, Yonghao Zhu, You Fu, Yangyang Jiang & Xiaoyu Hua

The World Health Organization states that early diagnosis is essential to increasing the cure rate for breast cancer, which poses a danger to women's health worldwide. However, the efficacy and cost limitations of conventional diagnostic techniques increase the possibility of misdiagnosis. In this work, we present a quantum hybrid classical convolutional neural network (QCCNN) based breast cancer diagnosis approach with the goal of utilizing quantum computing's high-dimensional data processing power and parallelism to increase diagnosis efficiency and accuracy. When working with large-scale and complicated datasets, classical convolutional neural network (CNN) and other machine learning techniques generally demand a large amount of computational resources and time. Their restricted capacity for generalization makes it challenging to maintain consistent performance across multiple data sets. To address these issues, this paper adds a quantum convolutional layer to the classical convolutional neural network to take advantage of quantum computing to improve learning efficiency and processing speed. Simulation experiments on three breast cancer datasets, GBSG, SEER and WDBC, validate the robustness and generalization of QCCNN and significantly outperform CNN and logistic regression models in classification accuracy. This study not only provides a novel method for breast cancer diagnosis but also achieves a breakthrough in breast cancer diagnosis and promotes the development of medical diagnostic technology.

Keywords Convolutional neural networks, Quantum computing, Quantum machine learning, Medical diagnostics, Breast cancer diagnostics

Breast cancer is one of the most common cancers in women worldwide and the second most common malignancy in the world after lung cancer. According to the global malignancy report published by Dr. Freddie Bray's team (2024), head of the Cancer Surveillance Unit of the International Agency for Research on Cancer (IARC), the number of new cases of female breast cancer worldwide is as high as 2,296,000, which accounts for 11.5% of all new cases of malignancy, second only to lung cancer, and ranks the second most common malignant tumor in the world[1]. This represents 11.5% of all new cases of malignant tumors and is second only to lung cancer as the leading cancer incidence in women worldwide. This figure indicates that more than 1 in 10 new cancer patients is a breast cancer patient[2]. Additional data show that breast cancer is one of the leading causes of cancer deaths in women between the ages of 40 and 55[3], and the National Breast Cancer Foundation suggests that early detection and treatment of breast cancer can significantly improve survival. For example, 5-year survival rates for localized breast cancer typically exceed 90%, while survival rates for advanced breast cancer are significantly lower. The high incidence of breast cancer and its significant impact on patients' quality of life make effective diagnostic techniques particularly important.

Machine learning and deep learning techniques have greatly advanced the field of image analysis in the last few decades[4–7]. Sapna Singh Kshatri et al.[8] have shown that convolutional neural networks excel in the analysis, preprocessing, segmentation, and data preparation of Magnetic Resonance Imaging (MRI) of the brain. Tariq Mahmood et al.[9] have delved into the application of active deep learning in medical image segmentation and classification, focusing on challenges in breast cancer images and proposing improvement strategies.

In addition, convolutional neural networks have shown great potential in areas such as new crown pneumonia detection[10], sentiment analysis[11], and computer vision[12]. Especially in the early detection and classification of breast cancer, convolutional neural network (CNN) has become one of the most important methods for breast cancer diagnosis with its excellent performance in medical image analysis[13].

College of Computer Science And Cyber Security(Pilot Software College), Chengdu University of Technology, Chengdu 610059, China. ✉email: lidongfen17@cdut.edu.cn

More and more research is devoted to the automatic detection and classification of breast cancer[14]. For example, Tariq Mahmood et al.[15] reviewed deep learning schemes for breast cancer diagnosis using multiple image modalities, highlighting the limitations of traditional machine learning methods and the potential of deep learning for improving diagnostic accuracy. Yan Pei et al.[16] proposed a mammography microcalcification detection method combining multi-scale features and radionics analysis, outperforming traditional machine learning models on the MIAS dataset. Yan Pei et al.[17] also developed a fully connected depth-separable convolutional neural network (FC-DSCNN) for detecting microcalcification clusters in mammograms, which outperformed traditional methods on the DDSM and PINUM datasets. Masud et al.[18] proposed using deep convolutional neural networks (DCNNs) for mammogram analysis to diagnose breast cancer. Parita Oza et al.[19] explored various convolutional neural network models to aid breast cancer diagnosis.

However, classical convolutional neural networks face the problem of insufficient arithmetic power when dealing with complex data structures, consume a large amount of computational resources, and require large-scale datasets for training. These limitations affect the accuracy and efficiency of conventional breast cancer diagnosis methods, especially with large-scale and complex data structures. Therefore, developing quick and precise diagnostic methods is crucial to improving early detection rates and treatment effectiveness for breast cancer.

With the emergence of quantum computing technology, its parallel processing capability, super computational power, and unique quantum superposition states allow computers to explore multiple computational paths simultaneously, thus enabling complex problems to be solved at unprecedented speeds when dealing with large-scale data and complex algorithms[20,21], and providing a new avenue in the development of medical diagnostics[22]. The combination of quantum computing and machine learning, known as quantum machine learning techniques, utilizes quantum state properties to enhance efficiency and accuracy through quantum data encoding, and quantum state preparation to enable precise manipulation of quantum states to execute algorithms.

Quantum machine learning techniques have shown potential in many applications[23–25]. For example, quantum support vector machines (QSVMs), quantum neural networks (QNNs), and quantum convolutional neural networks (QCNNs), which utilize quantum state representations and quantum gate operations to learn patterns and features of data, have received widespread attention as they exhibit high efficiency compared to traditional algorithms in solving complex problems[26–28]. Patrick Rebentrost et al.[29] demonstrated that quantum support vector machines (QSVMs) can obtain exponential speedups compared to traditional algorithms in certain tasks. Liu Jun-Hua et al.[30] showed that QCCNN can efficiently perform classification tasks. Bayro-Corrochano, Eduardo et al.[31] presented quaternion-based quantum neural networks (QQNNs) and demonstrated their applicability in robot control and pattern recognition in their study.

Despite these advances, the application of quantum machine learning techniques in medical diagnostics is still in its infancy, especially in breast cancer diagnostics, which has not been fully explored. Obtaining suitable datasets for machine learning experiments is often challenging, especially for medical data, due to privacy, confidentiality, security, and ethical issues[32]. Fortunately, some breast cancer diagnostic datasets have recently become benchmark datasets for breast cancer detection and classification studies[33] and are available for online access in the Kaggle machine learning repository along with other relevant data[34].

This study proposes a new breast cancer diagnostic method, the quantum hybrid convolutional neural network (QCCNN), aiming to fill the existing technological gap. The QCCNN combines the advantages of classical convolutional neural networks and quantum computing techniques, aiming to achieve higher diagnostic accuracies through improved computational efficiency. Through validation on different breast cancer datasets, the advantages of QCCNN over classical CNN and logistic regression models in terms of accuracy and computational efficiency are demonstrated, providing a new approach to the field of breast cancer as well as the broader field of medical diagnosis.

This paper anticipates that the proposed QCCNN method will be an important advancement in the field of breast cancer diagnosis. Improving the accuracy and efficiency of diagnosis, will enable early detection of breast cancer, assist physicians to better formulate treatment plans, increase patient survival and improve prognostic outcomes.

The main contributions of this paper are as follows:

1. A hybrid model, QCCNN, combining classical convolutional neural network and quantum computing techniques, is proposed.
2. The advantages of QCCNN in breast cancer diagnosis over traditional methods in terms of accuracy and computational efficiency are verified.
3. The potential applications and challenges of quantum machine learning in medical diagnosis are analyzed. The paper is structured as follows: Sect. "Materials and method" details the datasets, methods, and experimental design; Sect. "Results" presents the results; Sect. "Discussion" discusses the findings; and Sect. "Conclusions" concludes and outlines future research directions.

Materials and method

The application of Quantum Hybrid Classical Convolutional Neural Network (QCCNN) in the diagnosis of breast cancer is the primary focus of this work. For classification tasks, the German Breast Cancer Study Group (GBSG), the SEER breast cancer dataset, and the Wisconsin Diagnostics for Breast Cancer (WDBC) dataset were used as input data for the QCCNN, CNN, and logistic regression models, respectively. Comparing the diagnostic accuracy of these three models among the three datasets allowed for the validation of QCCNN's performance in the diagnosis of breast cancer. The models' process for diagnosing breast cancer is shown in Fig. 1.

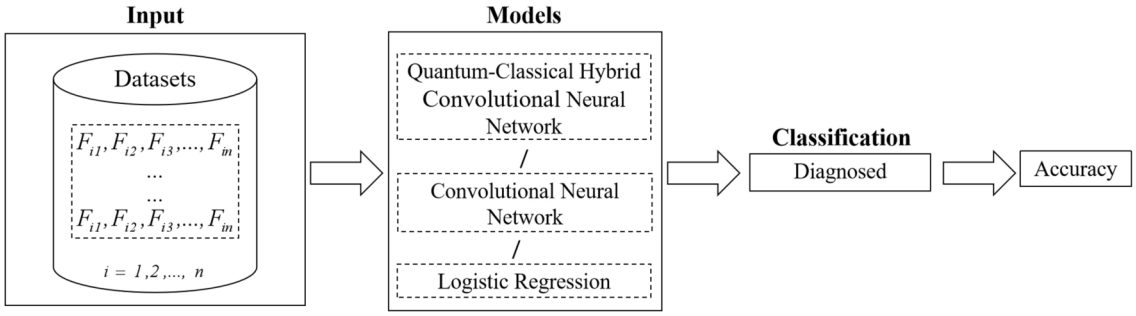

Fig. 1. Flowchart of breast cancer diagnosis for the model.

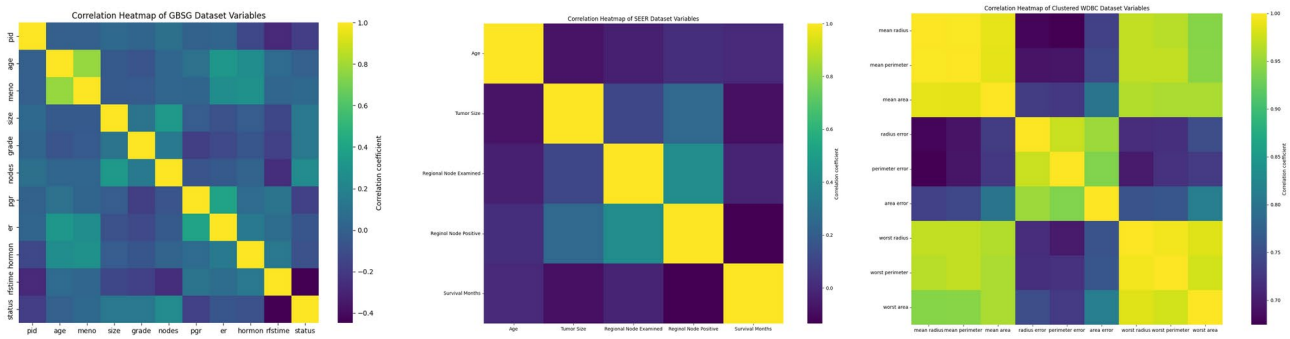

(a) GBSG Dataset **(b)** SEER Dataset **(c)** SEER Dataset

Fig. 2. To analyze the correlation between features in the dataset, we computed the Pearson's correlation coefficient matrix between the features and used this matrix to generate a heat map. Each cell in the heatmap represents the correlation between two features, with the color shade reflecting the strength of the correlation.

Datasets

The Kaggle website (a machine learning repository) provided the breast cancer diagnosis GBSG dataset, SEER dataset, and WDBC dataset used in this study. Figure 2 shows the association between feature variables in the dataset.

The German Breast Cancer Study Group (GBSG) conducted a trial including 720 patients with node-positive breast cancer between 1984 and 1989. Of those patients, 686 had complete prognostic variable data. These patient records are included in the GBSG dataset. The dataset has 11 distinctive features and 686 samples in its format. You may find a thorough explanation of this dataset in reference[35].

The population-based cancer statistics in the SEER dataset are sourced from the NCI's SEER program, which was updated in November 2017. The dataset covers female patients with invasive breast cancer diagnosed between 2000 and 2017. The dataset contains 4024 samples and 16 characteristic variables. Detailed information on this dataset can be found in the literature[36].

The WDBC dataset contains digitized images of breast cancer masses acquired by fine needle aspiration (FNA) from which tumor features have been calculated. The dataset contains 30 features, 10 of which are real features calculated based on the geometry of the cell nucleus boundaries in the image. The dataset has 569 samples. A detailed description and explanation of the WDBC dataset can be found in reference[37].

Data processing

In the research process, due to the differences in the magnitude and value range of each feature in the dataset. To eliminate the effect of these differences on the model training, this study adopted normalization, we chose to implement the Normalize function in Python's Scikit-learn library, which maps the normalized feature values to the π range $[-\pi, \pi]$, this is achieved by multiplying by a factor π, the formulae used for normalization are provided in Equation (1), where X represents the original data matrix, The Normalize function is applied to each feature, along axis 0, and the *norm = 'max'* parameter instructs the function to use the maximum value normalization method.

In this way, the maximum absolute value of each feature is scaled to π, and the minimum value is scaled to $-\pi$. This target range was chosen because it provides a uniform and bounded interval of values for subsequent data processing and analysis.

$$X_{norm} = \pi \cdot normalize(X, axis = 0, norm =' max') \quad (1)$$

Dataset	Sample size	Training set	Validation set
GBSG	686	480	206
SEER	4024	2817	1207
WDBC	569	398	171

Table 1. Size and division of the GBSG, SEER and WDBC datasets. The first column shows the name of each dataset, the second column indicates the total number of samples, the third column indicates the training set sample size and the fourth column indicates the validation set sample size.

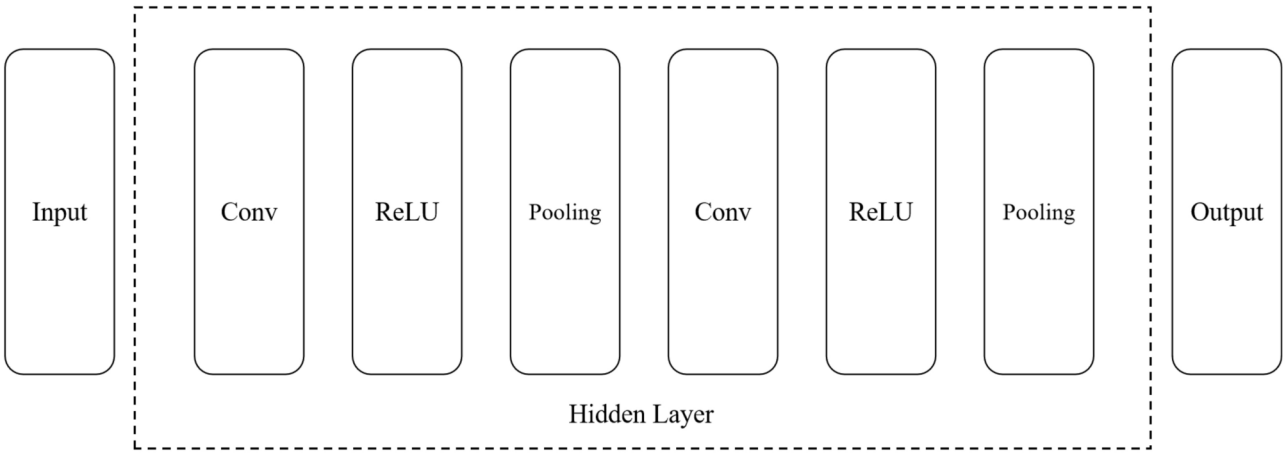

Fig. 3. A complete CNN structure.

After completing the data preprocessing, we divided the original dataset and used 70% of it as the training set for model training, while the remaining 30% was used as the validation set for evaluating the model performance. When dividing the dataset, we ensured that the distribution of samples in the training and validation sets was consistent with the original dataset. This step provides a solid foundation for subsequent model training and evaluation and provides a reliable guarantee for the generalization ability of the model. Table 1 demonstrates the size and division of each dataset.

Convolutional neural networks (CNN)

The structure of convolutional neural network (CNN) is similar to traditional neural networks, but the main difference is that it introduces convolutional and pooling layers[38]. In CNN, it usually includes an input layer, convolutional layer, activation layer, pooling layer, fully connected layer and output layer. The convolutional, activation, and pooling layers are often collectively referred to as the hidden layer. CNN is a deep learning model that is widely used in image processing and pattern recognition. Its workflow is as follows: first, the input image is passed through one or more convolutional layers, each of which consists of multiple filters (or convolutional kernels). These filters perform convolutional operations on the image by sliding windows over it to extract local features of the image. The structure of a complete convolutional neural network is shown in Fig. 3.

In this experiment Convolutional Neural Networks (CNN) has been used for the classification task on three different breast diagnostic datasets, also the classification accuracy is used as an evaluation criterion to compare with the results of QCCNN.The structural flow of the CNN model is shown in Fig. 4.

CNN model architecture

The Convolutional Neural Networks (CNN) model used in this study uses the following architecture:

- **Input layer:** the input data is a single channel, $I \in R^{H \times W \times l}$, where H and W represent the height and width of the input data.
- **Convolutional layer 1:** the first convolutional layer consists of K_1 convolutional kernels. The convolutional operation is defined in Eq. (2):

$$F_1 = ReLu(I * K_1 + b_1) \tag{2}$$

where * denotes the convolution operation and b_1 is the bias term.

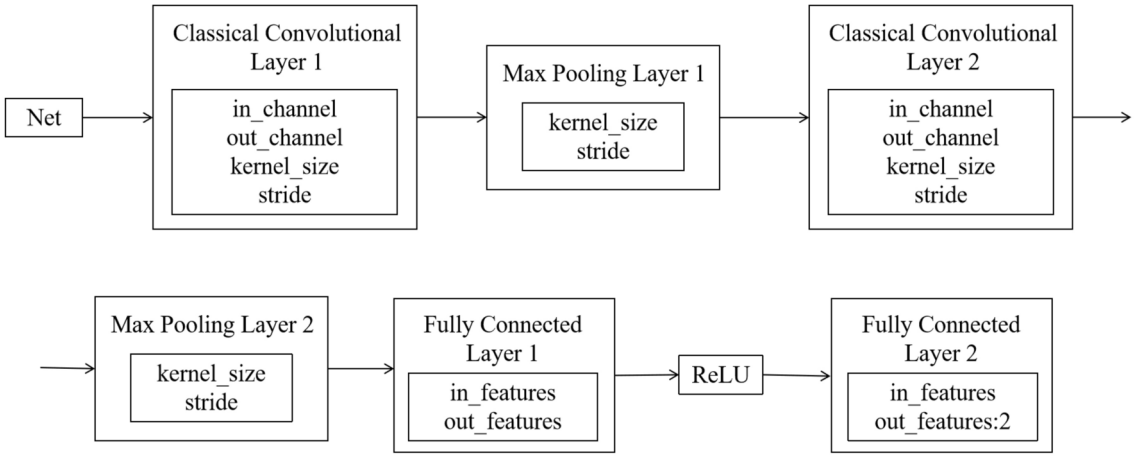

Fig. 4. Flowchart of the structure of the CNN model.

- **Maximum pooling layer 1:**the maximum pooling layer uses a $n \times n$ pooling kernel with a step size of s and no padding, and the operation is defined as in Eq. (3):

$$P_1 = max(F_1) \tag{3}$$

-
- **Convolutional layer 2:**the second convolutional layer has the same number of convolutional kernels as the first, $K_2 = K_1$.
- **Maximum pooling layer 2:** same as Maximum Pooling Layer 1 to further reduce the spatial size of the feature map.
- **Fully connected layer 1:** spreads the outputs of convolution and pooling layers and maps the features to D dimensions through a fully connected layer, the operation is defined as in Eq. (4):

$$F_2 = ReLU(P_2 \cdot W_1 + b_2) \tag{4}$$

where W_1 is the weight matrix and b_2 is the bias term.

- **Fully connected layer 2:**the final classification layer maps D -dimensional features to 2-dimensional outputs, with operations defined as in Eq. (5):

$$\hat{Y} = W_2 \cdot F_2 + b_3 \tag{5}$$

where $\hat{Y}$ is the predicted output and W_2 and b_3 are the weights and bias terms.

Quantum classical hybrid convolutional neural networks (QCCNN)

Quantum-classical hybrid convolutional neural network (QCCNN) is a neural network architecture that integrates quantum and classical computing[39]. The model is designed to make up for the shortcomings of classical convolutional neural networks (CNNs) in dealing with certain complex problems and to take full advantage of both classical and quantum computing to bring new possibilities in fields such as image recognition.

The experiments use the PennyLane quantum machine learning framework[40] to construct and implement a quantum-classical hybrid convolutional neural network (QCCNN) model, where the overall structure consists of a quantum convolutional layer and a fully connected layer, which are connected and work together on the input image to achieve efficient processing and accurate classification of the image.

A classification task was performed on three different breast diagnostic datasets to explore the potential feasibility of QCCNN in breast cancer diagnostic applications using classification accuracy as an evaluation criterion. The experiment simulated the complete data classification process of QCCNN, including data preprocessing, preparation of informative quantum states, and the complete QCCNN model consisting of a combination of quantum convolutional and classical fully connected layers. The structural flow of the model is shown in Fig. 5.

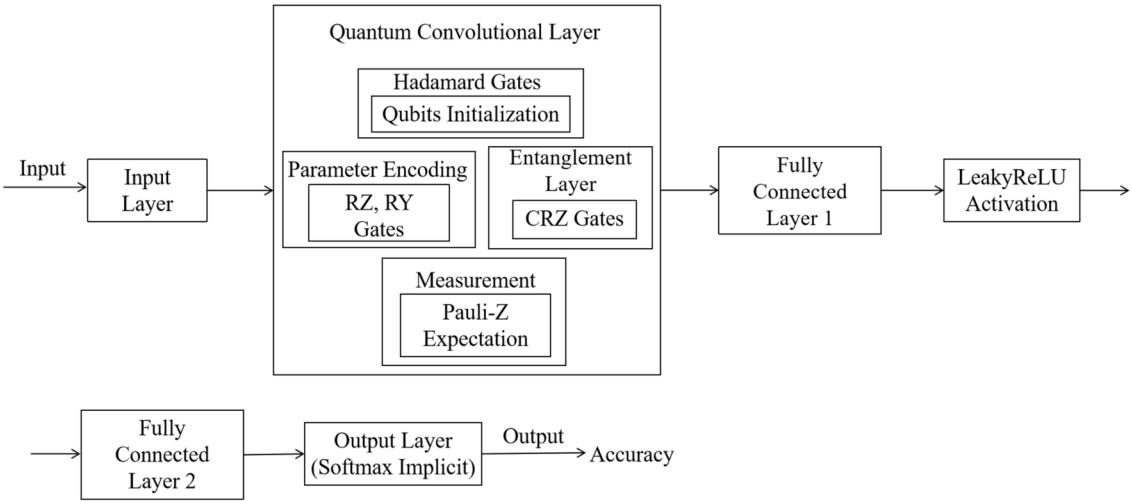

Fig. 5. Flowchart of the structure of the QCCNN model.

Quantum convolutional layer design
At the heart of the quantum convolutional layer is a parameterized quantum circuit that receives an input vector $x \in R^d$ and outputs the *Pauli-Z* expectation value of a set of quantum bits. The quantum circuit is designed as follows:

- **Initialization:** each qubit is initialized to the Hadamard ground state as in Eq. (6):

$$|H_i\rangle = \frac{1}{\sqrt{2}}(|0\rangle + |1\rangle) \tag{6}$$

-
- **Parametric encoding:** the input features are encoded into the quantum state through quantum gates. For each qubit, a coded gate $U(\theta)$ is used as in Eq. (7):

$$U(\theta) = \exp(-i\theta\sigma_x) \tag{7}$$

where θ are the parameters computed from the input features and σ_x is the *Pauli-X* matrix.

- **Quantum gate application:** in the circuit, for each layer 1, entanglement gate CR and single quantum bit gate RY are applied as in Eqs. (8) and (9):

$$CRZ(\Phi_{l,i}) = \exp\left(-i\Phi_{l,i}\sigma_z \bigotimes \sigma_z\right) \tag{8}$$

$$RY(\theta_{l,i}) = \exp(-i\theta_{l,j}\sigma_y) \tag{9}$$

where $\Phi_{l,i}$ and $\theta_{l,j}$ are the weight parameters of the circuit, σ_z and σ_y are the *Pauli-Z* and *Pauli-Y* matrices.

- **Expectation measurement:** the circuit output is the expectation value of the *Pauli-Z* operator for each qubit, as in Eq. (10):

$$E(Z_i) = \langle 0|U^\dagger Z_i U|0\rangle \tag{10}$$

where U is the unitary operator of the entire quantum circuit and Z_i is the *Pauli-Z* matrix of the *ith* qubit.

Classical neural network layer design
After the quantum convolution layer, the classical neural network layer further processes the features:

- **Fully connected layers:**the first fully connected layer maps the output z of the quantum convolution layer to an intermediate feature space as in Eq. (11):

$$h = W_{fc1Z} + b_{fc1} \tag{11}$$

where W_{fc1} and b_{fc1} are the weight matrix and bias vector of the fully connected layer.

- **LeakyReLU activation function:**he LeakyReLU activation function is applied to the output of the fully connected layer as in Eq. (12):

$$h_{LR} = LeakyReLU(h) \tag{12}$$

-
- **Output fully connected layer:**the final fully connected layer maps intermediate features to category probabilities as in Eq. (13):

$$y = softmax(W_{fc2}h_{LR} + b_{fc2}) \tag{13}$$

where W_{fc2} and b_{fc2} are the weights and biases of the output layer, the Softmax function converts the linear combination into a probability distribution.

Logistic regression

Experiments were conducted using a Logistic Regression model on three different breast diagnostic datasets for the classification task, and accuracy was also used as an evaluation criterion to compare with the results of QCCNN. Logistic regression is a widely used linear classification model that maps the input features to a probability value through a linear function that indicates the likelihood that the sample belongs to a specific category. The structural flow of the logistic regression model is shown in Fig. 6 and mathematically expressed as follows:

- **Linear combination:**the model computes a linear combination of input features *X* and weights *W*, plus *a* bias *b*, as in Eq. (14):

$$z = W^T X + b \tag{14}$$

-
- **Sigmoid function:**the result of the linear combination is mapped to the interval *(0, 1)* by the Sigmoid function to obtain the probability $\hat{y}$ as in Eq. (15):

$$\hat{y} = \frac{1}{1 + e^{-z}} \tag{15}$$

-

Logistic regression model architecture

The Logistic Regression model used in this study adopts the following architecture:

- **Input layer:** accepts a D-dimensional feature vector *X*.
- **Parameter layer:** contains *D* weight parameters *w* and *a* bias parameter *b*.

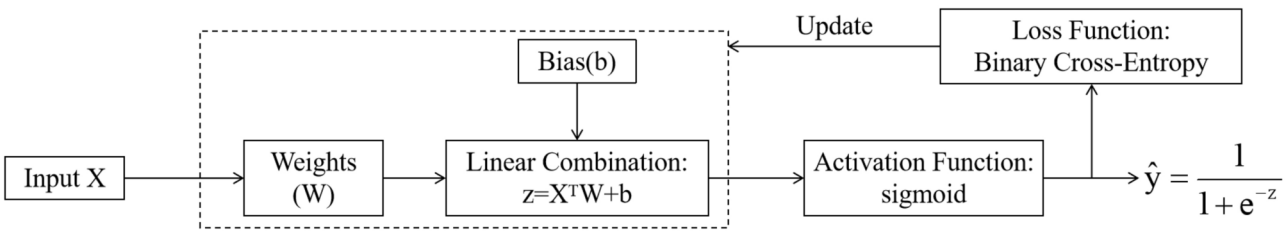

Fig. 6. Flowchart of the structure of the Logistic Regression model.

- **Output layer:** outputs $\hat{y}$, the probability that the input feature belongs to label *1*.

Experimental setup

Experimental setup for QCCNN and CNN models

In the experiment, we use the PyTorch framework to build and train the classical neural network part and integrate the PennyLane library to implement the quantum convolutional layer. The performance of the model will be evaluated by the accuracy ACC, which is calculated as in Eq. (16).

$$ACC = \frac{TP + TN}{TP + TN + FP + FN} \tag{16}$$

where *TP* is the number of true examples, *TN* is the number of true negative examples, *FP* is the number of false positive examples, and *FN* is the number of false negative examples.

The training process of the model follows the standard gradient descent algorithm with the following settings:

- **Learning rate:** set the initial learning rate to *0.1* for Adam optimizer.
- **Optimizer:** select the Adam optimizer to update the network weights and its update rule is shown in Eqs. (17, 18, 19):

$$m_t = \beta_1 m_{t-1} + (1 - \beta_1) \cdot \nabla_J(W) \tag{17}$$

$$V_t = \beta_2 v_{t-1} + (1 - \beta_2) \cdot (\nabla_J(W))^2 \tag{18}$$

$$W_{t+1} = W_t - \alpha \cdot \left(\frac{m_t}{\sqrt{v_t}} + \epsilon \right) \tag{19}$$

where m_t and v_t are the first-order and second-order moment estimates of the gradient, α are the learning rates, β_1 and β_2 are the adjustment coefficients, which ϵ are tiny constants added for numerical stability.

- **Loss function:**optimization is performed using the cross-entropy loss function L as in Eq. (20):

$$L(y, t) = -\sum_{i=1}^{C} t_i \log(y_i) \tag{20}$$

where *y* is the probability distribution predicted by the model, *t* is the one-hot encoding of the true labels, and *C* is the number of categories.

Experimental setup for the logistic regression model

In the experiment, we used the PyTorch framework[41] to construct and train Logistic Regression Model. The performance of the model is also evaluated by the accuracy rate, which is defined as the ratio of the number of correctly classified samples to the total number of samples. The following shows the training process of the model:

- **Initialization:**the weights *W* and bias b are initialized to *0*.
- **Optimizer:**the Adam optimizer is also used to update the parameters of the model and the learning rate is set to *0.01*.
- **Loss function:**Binary Cross-Entropy Loss is used to measure the difference between the probability distribution predicted by the model and the true labels, calculated as in Eq. (21).

$$L = -\frac{1}{N} \sum_{i=1}^{N} [y_i \cdot \log(\hat{y}_i) + (1 - y_i) \cdot \log(1 - \hat{y}_i)] \tag{21}$$

-

Results

To validate the feasibility and efficiency of the Quantum Hybrid Classical Convolutional Neural Convolutional Neural Network (QCCNN) used in this paper for breast cancer diagnostic applications, a Convolutional Neural Network (CNN) and Logistic Regression model were used for comparative analyses with the QCCNN. The performance of the models on the GBSG, SEER, and WDBC breast cancer diagnostic datasets, respectively, is also discussed in order to demonstrate the robustness and generalization of the QCCNN models. In the

Model	Training accuracy (%)	Validation accuracy (%)
QCCNN	<u>74.375</u>	<u>70.498</u>
CNN	59.708	58.944
Logistic regression	61.927	60.583

Table 2. Average accuracy of breast cancer diagnosis by each model on the GBSG dataset. The first column shows the name of each model, the second column indicates the diagnosis results of the model on the training set, and the third column indicates the diagnosis results of the model on the validation set. Underlined text indicates the best accuracy rate.

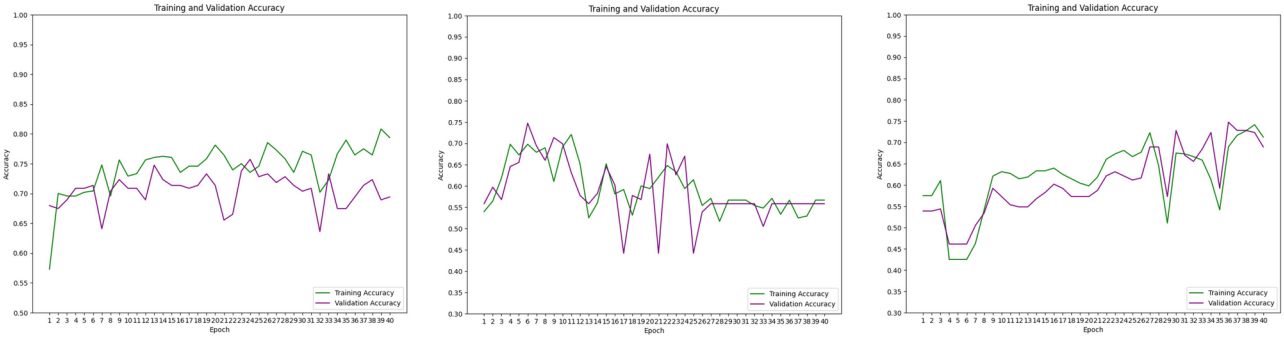

(a) Accuracy of QCCNN **(b)** Accuracy of CNN **(c)** Accuracy of Logistic Regression

Fig. 7. Accuracy graphs of QCCNN, CNN and Logistic Regression for breast cancer diagnosis on the GBSG dataset. Green indicates the accuracy of the model relative to the training set in each iteration, while purple indicates the accuracy relative to the validation set.

Model	Training Accuracy (%)	Validation Accuracy (%)
QCCNN	<u>89.544</u>	<u>90.088</u>
CNN	88.708	89.091
Logistic Regression	89.513	89.125

Table 3. Average accuracy of breast cancer diagnosis by each model on the SEER dataset. The first column shows the name of each model, the second column indicates the diagnosis results of the model on the training set, and the third column indicates the diagnosis results of the model on the validation set. Underlined text indicates the best accuracy rate.

experimental setup, 70% of each dataset was used as the training set and the remaining 30% as the validation set, and accuracy was chosen as the key metric to measure the diagnostic performance of the model.

Results on the GBSG dataset

Table 2 compares the average accuracies of different models trained on the GBSG dataset, with the best accuracies underlined. The results show that QCCNN has the best performance among all models with an average accuracy of 74.375% and 70.498% on the training and validation sets, respectively.

To further analyze the diagnostic effectiveness of the three models on the GBSG dataset, the diagnostic accuracies of each network on the training and validation sets are presented in Fig. 7. The highest accuracies of the QCCNN on the training and validation sets are 80.833% and 75.728%, respectively; in comparison, the highest accuracies of the CNN are 72.083% (for the training set) and 74.757% (for the validation set), and the logistic regression model has the highest accuracy of 74.167% (training set) and 74.757% (validation set). This shows that the highest accuracy of QCCNN is better than the other two models.

Combining the results in Table 2 and Fig. 7, QCCNN is the best for breast cancer diagnosis on the GBSG dataset.

Results on the SEER dataset

Table 3 compares the average accuracies of different models trained on the SEER dataset, with the best accuracies underlined. The results show that QCCNN has the best performance among all models with an average accuracy of 89.544% and 90.088% on the training and validation sets, respectively.

To further analyze the diagnostic effectiveness of the three models on the SEER dataset, the diagnostic accuracies of each network on the training and validation sets are illustrated in Fig. 8. The highest accuracy of

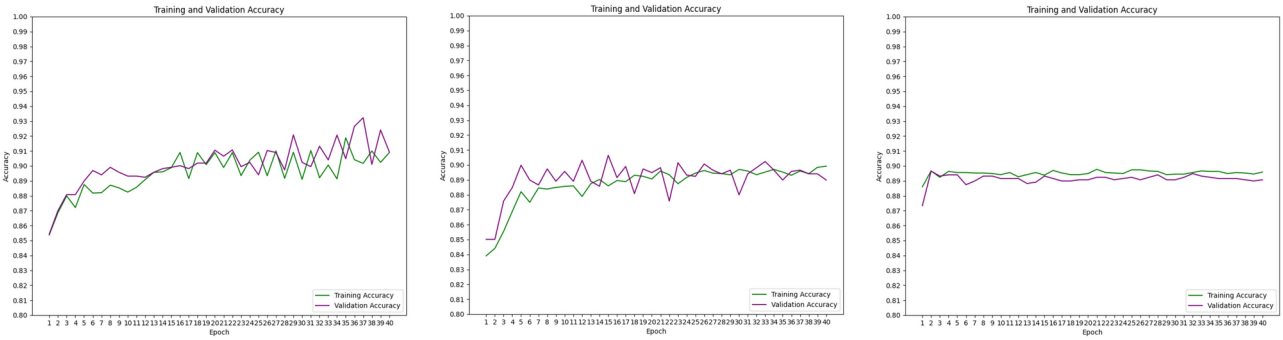

(a) Accuracy of QCCNN **(b)** Accuracy of CNN **(c)** Accuracy of Logistic Regression

Fig. 8. Accuracy graphs of QCCNN, CNN and Logistic Regression for breast cancer diagnosis on the SEER dataset. Green indicates the accuracy of the model relative to the training set in each iteration, while purple indicates the accuracy relative to the validation set.

Model	Training accuracy (%)	Validation accuracy (%)
QCCNN	<u>97.099</u>	<u>96.155</u>
CNN	92.932	92.822
Logistic regression	91.354	91.184

Table 4. Average accuracy of breast cancer diagnosis by each model on the WDBC dataset. The first column shows the name of each model, the second column indicates the diagnosis results of the model on the training set, and the third column indicates the diagnosis results of the model on the validation set. Underlined text indicates the best accuracy rate.

QCCNN on the training and validation sets is 91.885% and 93.232%, respectively; in comparison, the highest accuracy of CNN is 89.915% (for the training set) and 90.646% (for the validation set), and the highest accuracy of the logistic regression model has the highest accuracy of 89.773% (training set) and 89.652% (validation set). Obviously, the highest accuracy of QCCNN is better than the other two models.

Combining the results in Table 3 and Fig. 8, QCCNN has the best breast cancer diagnosis on the SEER dataset.

Results on the WDBC dataset

Table 4 demonstrates the average accuracies of different models trained on the WDBC dataset, with the best accuracies underlined. The results show that the average accuracy of QCCNN is 97.099% and 96.155% on the training and validation sets, respectively, which is significantly higher than that of CNN and logistic regression models.

To further evaluate the diagnostic performance of the three models on the WDBC dataset, the diagnostic accuracies of each network on the training and validation sets are presented in Fig. 9. The highest accuracy rates of QCCNN on the training and validation sets are 98.747% and 97.661%, respectively; in comparison, the highest accuracy rates of CNN are 96.742% (for the training set) and 97.076% (for the validation set), and the highest accuracy rate of logistic regression model has the highest accuracy of 94.710% (training set) and 94.737% (validation set). From the results, it can be seen that the highest accuracy of QCCNN is also better than the other two models.

Combining the results in Table 4 and Fig. 9, QCCNN is the best for breast cancer diagnosis on the WDBC dataset.

As a result, the QCCNN model proposed in this paper exhibits high accuracy in breast cancer diagnosis compared to the other two breast cancer diagnosis models. This result suggests that the approach of combining quantum computing with classical computing has significant potential for application in the field of medical image analysis and disease diagnosis.

Discussion

This study delves into the application of quantum machine learning techniques in breast cancer diagnosis. In order to make use of quantum computing and allow the network model to capture more complicated data properties, we used a quantum hybrid classical convolutional neural network (QCCNN), which adds a quantum convolutional layer on top of the classical convolutional neural network. Diagnostic analyses were performed on three different breast cancer datasets: GBSG, SEER, and WDBC. The results show that the generalization ability of the quantum approach in dealing with complex data exhibits significant advantages, which is consistent with the latest research in the field of current quantum computing and suggests that quantum computing has the potential to enhance the efficiency of machine learning tasks[42,43].

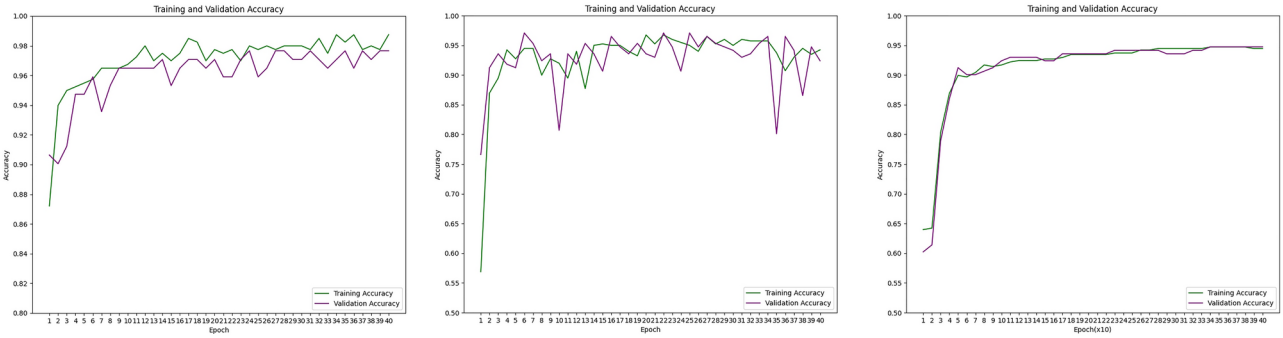

(a) Accuracy of QCCNN **(b)** Accuracy of CNN **(c)** Accuracy of Logistic Regression

Figure 9. Accuracy graphs of QCCNN, CNN and Logistic Regression for breast cancer diagnosis on the WDBC dataset. Green indicates the accuracy of the model relative to the training set in each iteration, while purple indicates the accuracy relative to the validation set.

During the experiments, not only the logistic regression model, classical convolutional neural network (CNN) and QCCNN are used to classify the three datasets, but also the key modules and structures designed for these models are described in detail. The quantum convolutional layer of QCCNN enhances the model's ability to extract the features of the data by the superposition and entanglement characteristics of the quantum states. Furthermore, the network gains a nonlinear transformation capacity with the addition of the quantum layer, which is not possible with conventional CNNs. The results show that the QCCNN significantly outperforms both the logistic regression model and the CNN in terms of classification accuracy. This result is similar to the best result reported by Fontes et al.[44], which further confirms the potential and application value of quantum methods in breast cancer diagnosis. The quantum convolutional layer and the conventional fully connected layer are merged to create a hybrid learning framework in the QCCNN model. When working with vast amounts of data, this approach not only makes use of the benefits of quantum computing but also maintains the stability of traditional neural networks. Meanwhile, the robustness and generalization of the QCCNN model are confirmed through testing on three distinct datasets, adding credence to its viability in real-world applications.

However, there are some limitations of this study.

The design of current quantum circuits has not yet fully taken into account the effects of noise in realistic Noisy Intermediate Scale Quantum (NISQ) environments, as studied by Erik B. Terres Escudero et al.[45], which may have an impact on the performance of the quantum model in practical applications. Future research could explore methods to assess the effect of noise in simulated real NISQ environments to more fully evaluate the performance and robustness of the model, or explore deeper levels of quantum circuits to further improve the performance of the model.

In addition, the experiments in this study were conducted on a conventional computer, and although GPUs are able to accelerate some of the computations, their computational speed for quantum circuits is not yet comparable to that of a real quantum computer (QPU), and the use of QPUs will be further explored in future studies to fully evaluate the performance of the QCCNN in practical applications.

Meanwhile, we plan to explore different model simplification and optimisation strategies to reduce the computational requirements while maintaining or improving the accuracy of the models to expand the application of quantum machine learning in medical diagnostics.

In summary, this study demonstrates the effectiveness of quantum machine learning in breast cancer diagnosis and provides a new perspective on the research field of combining quantum computing and machine learning. With the continuous progress of quantum technology, it is expected that quantum machine learning technology will play a greater role in future medical diagnosis.

Conclusion

In this study, we innovatively proposed a breast cancer diagnosis method based on quantum hybrid classical convolutional neural network (QCCNN) and verified its effectiveness in practical applications. The model was applied to three breast cancer datasets, GBSG, SEER and WDBC, and the classification performance was compared with that of classical convolutional neural network (CNN) and logistic regression models.

The results show that QCCNN performs the best in terms of classification accuracy in all cases, significantly outperforming both the logistic regression model and CNN, confirming its superior performance in breast cancer diagnosis. This further demonstrates the advantages of quantum computing in processing complex data and highlights the great potential of quantum machine learning techniques in medical diagnosis.

The limitations of this study are: Firstly, the current quantum circuit design was performed in an ideal state, and the specific effect of noise in the Noisy Intermediate Scale Quantum (NISQ) environment on the performance of the QCCNN model has not yet been explored in depth, which will be an important direction for future research. Secondly, although the experiments in this study were performed on a conventional computer where GPUs can accelerate some of the computations, there is still a gap compared to a true quantum computer (QPU), which is an area that needs to be expanded for future research.

Despite these limitations, the application of QCCNN models in breast cancer diagnosis is promising. With the development and optimization of quantum computing, the QCCNN model is expected to become a powerful tool in the field of medical diagnosis, providing doctors with more accurate and faster diagnostic results, thus helping patients to detect and treat diseases earlier.

Breast cancer staging is an important part of treatment, which is significant for the development of treatment plans and prognosis assessment. Therefore, applying the QCCNN model to the task of breast cancer staging will be an important expansion direction for future research. We expect to explore the performance of the QCCNN model on the breast cancer staging task through further research to provide more comprehensive and precise support for the clinical diagnosis and treatment of breast cancer.

In addition, QCCNN being a computationally intensive model, assessing its computational efficiency and complexity is critical to determine its applicability in real-time clinical settings. Future research needs to further explore the use of QPU to more fully assess the computational efficiency of the model and explore how its complexity affects its performance in real-world applications.

To further promote the research and application of quantum machine learning techniques in the field of medical diagnosis, future research considers a comprehensive performance evaluation of models, including but not limited to training time, prediction speed, and ROC and AUC metrics, as well as an in-depth exploration of diversified quantum technologies and innovative approaches to optimize model performance. These efforts will not only broaden the application scenarios of quantum machine learning technology but may also bring revolutionary advances in the field of medical diagnosis.

Data availability

The data are available from the corresponding author on reasonable request.The dataset used for the experiment is available at https://www.kaggle.com/datasets/sahilnbajaj/cancer-classification.

Received: 31 May 2024; Accepted: 30 September 2024
Published online: 21 October 2024

References

1. Briguglio, G. *et al.* Polyphenols in cancer prevention: New insights. *Int. J. Funct. Nutr.* **1**, 1. https://doi.org/10.3892/ijfn.2020.9 (2020).
2. Xi, Z. *et al.* Interpretation on the report of global cancer statistics 2022. *Chin. J. Oncol.* **46**, 710–721. https://doi.org/10.3760/cma.j.cn112152-20240416-00152 (2024).
3. DeSantis, C.-E. *et al.* Breast CA-NCER statistics. *CA Cancer J. Clin.* **69**, 438–451. https://doi.org/10.3322/caac.21583 (2019).
4. Sarvamangala, D.-R. & Kulkarni, R.-V. Convolutional neural networks in medical image understanding: A survey. *Evolut. Intell.* **15**, 1–22. https://doi.org/10.1007/s12065-020-00540-3 (2022).
5. Mehta, A.-K., Swarnalatha, R., Subramoniam, M. & Salunkhe, S. A convolutional neural network for covid-19 diagnosis: An analysis of coronavirus infections through chest x-rays. *Electronics* **11**, 3975. https://doi.org/10.3390/electronics11233975 (2022).
6. Pacal, I. Maxcervixt: A novel lightweight vision transformer-based approach for precise cervical cancer detection. *Comput. Vis. Image Underst.* **184**, 103021. https://doi.org/10.1016/j.cviu.2023.103021 (2024).
7. Pacal, I. A novel swin transformer approach utilizing residual multi-layer perceptron for diagnosing brain tumors in MRI images. *Int. J. Mach. Learn. Cybern.* **15**, 3579–3597. https://doi.org/10.1007/s13042-024-02110-w (2024).
8. Kshatri, D. S. & Singh, S. Convolutional neural network in medical image analysis: A review. *Arch. Comput. Methods Eng.* **30**, 2793–2810 (2023).
9. Mahmood, T., Rehman, A., Saba, T., Nadeem, L. & Bahaj, S. A. O. Recent advancements and future prospects in active deep learning for medical image segmentation and classification. *IEEE Access* **11**, 113623–113652. https://doi.org/10.1109/ACCESS.2023.3313977 (2023).
10. Sarki, R., Ahmed, K., Wang, H., Zhang, Y.-C. & Wang, K. Automated detection of covid-19 through convolutional neural network using chest x-ray images. *PLOS ONE* **17**, e0262052 (2011).
11. C.-D. Santos, M. G. Deep convolutional neural networks for sentiment analysis of short texts. in *Proceedings of COLING 2014, The 25th International Conference on Computational Linguistics: Technical Papers*, pp. 69–78 (2014).
12. Zhao, X. *et al.* A review of convolutional neural networks in computer vision. *Artif. Intell. Rev.* **57**, 1–43 (2024).
13. Işık, G. & İshak, P. Few-shot classification of ultrasound breast cancer images using meta-learning algorithms. *Neural Comput. Appl.* **36**, 12047–12059 (2024).
14. Coşkun, D. *et al.* A comparative study of yolo models and a transformer-based yolov5 model for mass detection in mammograms. *Turk. J. Electr. Eng. Comput. Sci.* **31**, 10. https://doi.org/10.55730/1300-0632.4048 (2023).
15. Mahmood, T. *et al.* A brief survey on breast cancer diagnostic with deep learning schemes using multi-image modalities. *IEEE Access* **8**, 165779–165809. https://doi.org/10.1109/ACCESS.2020.3021343 (2020).
16. Mahmood, T. *et al.* An automatic detection and localization of mammographic microcalcifications ROI with multi-scale features using the radiomics analysis approach. *Cancers* **13**, 5916. https://doi.org/10.3390/cancers13235916 (2021).
17. Rehman, K. U. *et al.* Computer vision-based microcalcification detection in digital mammograms using fully connected depthwise separable convolutional neural network. *Sensors* **21**, 4854. https://doi.org/10.3390/s21144854 (2021).
18. Oza, P., Sharma, P., Patel, S. & Kumar, P. Deep convolutional neural networks for computer-aided breast cancer diagnostic: A survey. *Neural Comput. Appl.* **34**, 1815–1836 (2022).
19. Masud, M., Rashed, A. E. E. & Hossain, M. H. Convolutional neural network-based models for diagnosis of breast cancer. *Neural Comput. Appl.* **34**, 11383–11394 (2022).
20. Kanamori, Y. & Yoo, S.-M. Quantum computing: Principles and applications. *J. Int. Technol. Inf. Manag.* **29**, 43–71 (2020).
21. Bu, K.-F. Quantum computing meets federated learning. *Sci. China Phys. Mech. Astron.* **65**, 210331. https://doi.org/10.1007/s11433-021-1788-3 (2022).
22. Maximillian, Z. *et al.* Quantum computing's potential for drug discovery: Early stage industry dynamics. *Drug Discov. Today* **26**, 1680–1688 (2021).
23. Peral-García, D., Cruz-Benito, J. & García-Penalvo, F. J. Systematic literature review: Quantum machine learning and its applications. *Comput. Sci. Rev.* **51**, 100619 (2024).
24. Innan, N., Bennai, M. & Khan, M.-A. Financial fraud detection: A comparative study of quantum machine learning models. *Int. J. Quant. Inf.* **22**, 2350044. https://doi.org/10.1142/S0219749923500442 (2024).
25. Rithvik, G. Computational identification of inhibitors of msut-2 using quantum machine learning and molecular docking for the treatment of alzheimer's disease. *Alzheimer's Dement.* **17**, e049671. https://doi.org/10.1002/alz.049671 (2021).

26. Suzuki, T., Miyazaki, T. & Hasebe, T. Quantum support vector machines for classification and regression on a trapped-ion quantum computer. *Quant. Mach. Intell.* **6**, 31. https://doi.org/10.1007/s42484-024-00165-0 (2024).
27. Khan, A.R.-K. & Tariq, M. Machine learning: Quantum vs classical. *IEEE Access* **8**, 219275–219294 (2020).
28. Maheshwari, D., Sierra-Sosa, D. & Garcia-Zapirain, B. Quantum machine learning applications in the biomedical domain: A systematic review. *IEEE Access* **10**, 80463–80484 (2022).
29. Rebentrost, P., Lloyd, S. & Mohseni, M. Quantum support vector machine for big data classification. *Phys. Rev. Lett.* **113**, 130503. https://doi.org/10.1103/PhysRevLett.113.130503 (2014).
30. Liu, J.-H. *et al.* Hybrid quantum-classical convolutional neural networks. *Sci. China Phys. Mech. Astron.* **64**, 290311 (2021).
31. Bayro-Corrochano, E., Solis-Gamboa, S., Altamirano-Escobedo, G., Lechuga-Gutierres, L. & Lisarraga-Rodriguez, J. Quaternion spiking and quaternion quantum neural networks: Theory and applications. *Int. J. Neural Syst.* **31**, 2050059. https://doi.org/10.1142/S0129065720500598 (2021) (**PMID: 32938264**).
32. Hollis, K. F. To share or not to share: Ethical acquisition and use of medical data. *AMIA Summits Transl. Sci. Proc.* **2016**, 420 (2016).
33. Mangasarian, O.-L. Pattern recognition via linear programming: Theory and applications to medical diagnosis. *Large-scale Numerical Optimization* 22–30 (1990).
34. Banachewicz, K. & Massaron, L. *The Kaggle Book: Data Analysis and Machine Learning for Competitive Data Science* (Packt Publishing Ltd, 2022).
35. Royston, P. & Altman, D. G. External validation of a cox prognostic model: Principles and methods. *BMC Med. Res. Method.* **13**, 1–15. https://doi.org/10.1186/1471-2288-13-33 (2013).
36. Teng, J. Seer breast cancer data. *IEEE Dataport*[SPACE]https://doi.org/10.21227/a9qy-ph35 (2019).
37. Dora, L., Agrawal, S., Panda, R. & Abraham, A. Optimal breast cancer classification using gauss-newton representation-based algorithm. *Expert Syst. Appl.* **85**, 134–145. https://doi.org/10.1016/j.eswa.2017.05.035 (2017).
38. Schmidhuber, J. Deep learning in neural networks: An overview. *Neural Netw.* **61**, 85–117 (2015).
39. Andrea, M., Maureen, M., Miriam, L. J., Balthasar, S. & Thomas, M. Quantum-classical convolutional neural networks in radiological image classification. *2022 IEEE International Conference on Quantum Computing and Engineering (QCE)* (2022).
40. Schuld, M., Bergholm, V., Gogolin, C., Izaac, J. & Killoran, N. Pennylane: Automatic differentiation of hybrid quantum-classical computations. *Quantum* **2**, 56 (2018).
41. Paszke, A., Gross, S. & Francisco Massa, E. A. Pytorch: An imperative style, high-performance deep learning library. *Adv. Neural Inf. Process. Syst.* **32** (2019).
42. Havlíček, V. *et al.* Supervised learning with quantum-enhanced feature spaces. *Nature* **567**, 209–212 (2019).
43. Biamonte, J. et al. Quantum machine learning. *Nature* **549**, 195–202 (2017).
44. Pereira Fontes, J.-P., Lopez, M. A. G. Representation learning approach to breast cancer diagnosis. *ECR 2019, European Congress of Radiology* (2019).
45. Escudero, E. T., Alamo, D. A. & O. M. Gómez, P. G. B. Assessing the impact of noise on quantum neural networks: An experimental analysis. *International Conference on Hybrid Artificial Intelligence Systems* 314–325, https://doi.org/10.1007/978-3-031-40725-3_27 (2023).

Acknowledgements

This work was supported in part by the National Natural Science Foundation of China (Grant Nos: 62172060) and National Key R&D Program of China (Grant Nos: 2022YFB3304303).

Author contributions

All authors developed the idea and the theory. D.L. responsible for the overall direction of the project. All authors contributed to the discussions and interpretations of the results and wrote the manuscript.

Declarations

Competing interests

The authors declare no competing interests.

Additional information

Correspondence and requests for materials should be addressed to D.L.

Reprints and permissions information is available at www.nature.com/reprints.

Publisher's note Springer Nature remains neutral with regard to jurisdictional claims in published maps and institutional affiliations.

Open Access This article is licensed under a Creative Commons Attribution-NonCommercial-NoDerivatives 4.0 International License, which permits any non-commercial use, sharing, distribution and reproduction in any medium or format, as long as you give appropriate credit to the original author(s) and the source, provide a link to the Creative Commons licence, and indicate if you modified the licensed material. You do not have permission under this licence to share adapted material derived from this article or parts of it. The images or other third party material in this article are included in the article's Creative Commons licence, unless indicated otherwise in a credit line to the material. If material is not included in the article's Creative Commons licence and your intended use is not permitted by statutory regulation or exceeds the permitted use, you will need to obtain permission directly from the copyright holder. To view a copy of this licence, visit http://creativecommons.org/licenses/by-nc-nd/4.0/.

© The Author(s) 2024